Front. Phys. 11(2), 115204 (2016)
DOI 10.1007/s11467-016-0567-4

REVIEW ARTICLE

Survey of plasmonic gaps tuned at sub-nanometer scale in self-assembled arrays

Li-Hua Qian[1,2,*], Li-Zhi Yi[1], Gui-Sheng Wang[1], Chao Zhang[1,2], Song-Liu Yuan[1,†]

[1] *School of Physics, Huazhong University of Science and Technology, Wuhan 430074, China*
[2] *Flexible Electronics Center, Huazhong University of Science and Technology, Wuhan 430074, China*
*Corresponding authors. E-mail: *lhqian@hust.edu.cn, †yuansl@hust.edu.cn*

Received December 18, 2015; accepted January 25, 2016

Creating nanoscale and sub-nanometer gaps between noble metal nanoparticles is critical for the applications of plasmonics and nanophotonics. To realize simultaneous attainments of both the optical spectrum and the gap size, the ability to tune these nanoscale gaps at the sub-nanometer scale is particularly desirable. Many nanofabrication methodologies, including electron beam lithography, self-assembly, and focused ion beams, have been tested for creating nanoscale gaps that can deliver significant field enhancement. Here, we survey recent progress in both the reliable creation of nanoscale gaps in nanoparticle arrays using self-assemblies and in the in-situ tuning techniques at the sub-nanometer scale. Precisely tunable gaps, as we expect, will be good candidates for future investigations of surface-enhanced Raman scattering, non-linear optics, and quantum plasmonics.

Keywords surface plasmon, tunable, plasmonic gap, quantum plasmon, surface-enhanced Raman scattering, self-assembly, nanoparticle array

PACS numbers 52.25.Tx, 64.75.Yz

Contents

1 Overview of plasmonics

Light-metal interactions were well exploited in a number of ancient artworks that are now on display around the world. One of the most common examples is the colorful window glass found in many ancient European churches, where the colors actually are a result of the scattering of metallic nanoparticles (NPs) [1]. Another even more famous example is the Lycurgus cup, which shows a strikingly red color when viewed in transmitted light, but turns green in reflected light, as shown in Fig. 1(a) [2]. This remarkable, dichroic mystery was unveiled after Mie theoretically solved Maxwell's equations for a plane wave-particle configuration [3]. The simulated cross section of scattering as illustrated in Fig. 1(b) shows the coherent tendency of the absorption spectrum measured experimentally. Essentially, this phenomenon, created by surface plasmon polaritons (SPPs), is attributed to the fact that metallic nanostructures (such as Au, Cu, and Ag) support coherent oscillations of conduction electrons in response to incident light, leading to significantly enhanced electromagnetic fields at the surface and opening up new opportunities in plasmonics and nanophotonics [4]. The experimental evidence of SPP standing waves in metallic films were obtained by Kretschman and Otto [5]. Meanwhile, the planar metallic film supporting the SPP is extremely sensitive to its surrounding dielectrics; this property is widely utilized in biological sensors [6]. With the rapid advances of nanofabrication techniques and microscopic spectrophotometers over the past decades [7–9], proposed uses have been extended to include many new applications, particularly plasmonic rulers [10], surface-enhanced spectroscopy [11, 12], optical waveguides [13], nanolasers [14], and optical modulators [15]. Nowadays, the ability to manipulate and characterize light at the nanometer scale permits the fabrication of subwavelength optical devices. In these devices, optical components potentially can be miniaturized so they are comparable in size to their electronic

*Special Topic: Frontiers of Plasmonics (Ed. Hong-Xing Xu).

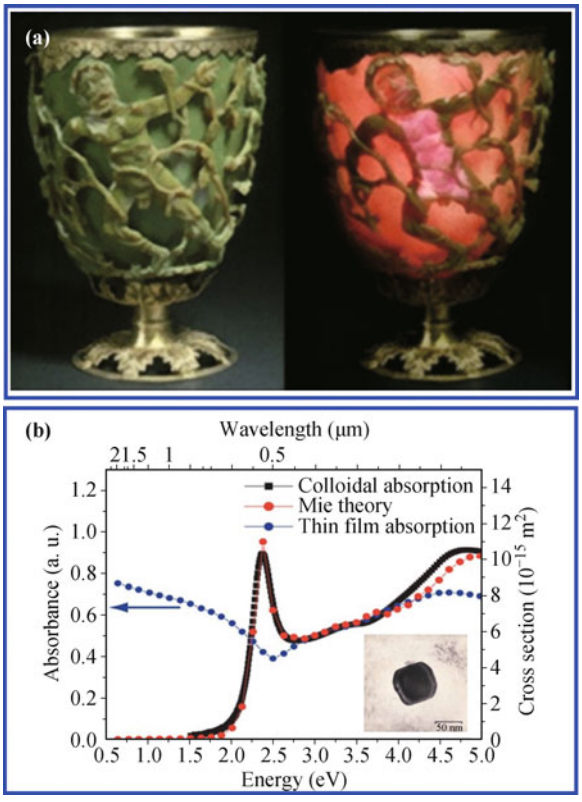

Fig. 1 The Lycurgus cup concealing light-metal interactions. **(a)** Lycurgus cup showing a striking green color when viewed in reflection, but looking red in transmitted light. **(b)** Absorption spectrum of an aqueous solution of 30 nm Au colloids (black dots) showing good agreement with the calculated spectrum according to Mie theory (red dots). Data of a thin film are represented for comparison. Inset in Fig. 1(b) displaying the scanning electron microscopy image of a typical NP embedded in the glass. Reproduced with permission from Ref. [2].

counterparts [16, 17]. Therefore, plasmonics holds great promise for penetration into chemical and biological sensors at tiny volumes, even more so than optoelectronic nanodevices were initially anticipated to accomplish [18, 19].

2 Plasmonic gaps created by self-assembly

Due to strong near-field coupling, the intense electromagnetic field within the plasmonic gaps stimulates continuous development in several disciplines. Surface-enhanced Raman scattering (SERS) [20], nonlinear optics [21], hot electron mediated chemistry [22], and quantum plasmonics [23] have been studied in the past decade. For SERS substrates, these gaps can serve as "hot spots," where the detection of very few molecules has been experimentally realized. Nonlinear optics has been reported upon in several coupling configurations, such as NP-film systems [24], NP-nanowires [25], NP chains [26], nanorod dimers [27], NP dimers [28], and NP prisms [29]. In order to consider quantum plasmonics, gaps less than 1 nm are investigated to clarify the photon-induced electron tunneling between neighboring nanoparticles. However, the classical electrodynamics model breaks down when the gap enters the sub-nanometer (sub-nm) region, where electron tunneling disturbs the interaction between the surface plasmons [30]. Quantum mechanical calculations indicate that plasmon bands exhibit gradual redshifts with shrinking gap transitions and blueshifts when quantum effects and charge transfers dominate the interactions among the neighboring nanoparticles. An NP cluster with sub-nm scale gaps, especially NP dimers, becomes an ideal plasmonic substrate for experimental and theoretical studies. Even a dramatic color change can be observed in NP arrays where the gaps can be controlled by applying several methodologies [31–33].

The first method involves random aggregations triggered by some extraneous chemicals, including molecules, DNA, and ions, which can interrupt the surface charging onto metal NPs. When the suitable molecules or ions are added to the metallic colloids, a color change is visible to the naked eye [34–37]. Partial aggregations of gold colloids give rise to some plasmonic gaps, inducing the output of the SERS with extraordinarily large enhancements [38, 39]. When plasmonic NPs are assembled at the two immiscible phases and even aggregated into volume colloids [40], the spatial distribution of the NPs can be tailored by changing their chemical environments [41, 42]. A stepwise strategy to generate regular heterogeneous binary NP arrays has also been reported in the literature [43]. Nowadays, based on this principle of random aggregation, gold colloids have become commercially available in products used as biological detectors, such as oviposit and pregnancy test strips.

In the second method, similar to the formation of a "coffee ring", a two-dimensional NP array can be achieved by self-assembly on a liquid/air interface [44]. The NP within the colloid will flow towards the contact line in order to compensate for the volume lost during the solvent's evaporation [45]. Sequential convection will induce spontaneous organization of NPs in the vicinity of the contact line. As such, this process is referred to as convective assembly; it is usually utilized to assemble micron-scale spheres where the limited confinement of colloidal volume is involved.

To make this assembling technique applicable for fabricating well-defined NP arrays, local confinements of colloidal volume during the evaporation of solvents is normally necessary; several attempts were made to achieve this. The self-assembly method by Kim *et al.*, for in-

stance, enabled the creation of two-dimensional and three-dimensional colloidal crystal films by confining very small amounts of colloidal suspension within two parallel glass sheets as shown in Fig. 2(a) and Fig. 2(b). This method can be used to assemble not only high-quality colloidal crystals with a diameter on the submicron scale, but also monolayered and multilayered colloidal crystals over a large substrate [46]. Hong *et al.* described a robust method that capitalizes on imposed axially symmetrical geometries to control the solvent evaporations as shown in Figs. 2(c)–(d). The capillary flow and evaporative processing of microfluids are confined below the indenters with various geometries. The indenters direct the formation of a variety of complex, highly regular surface patterns in a precisely controllable manner [47]. In our previous investigations, an assembly technique that resembles the writing action of a "pipette pen" was developed by confining the colloid at the edge of the pipette. Gold NP arrays can be obtained by controlling the assembling parameters; each strip of these gold NP arrays has a width on the micron scale; they are closely packed in a hexagonal arrangement with interparticle distances smaller than 3 nm in the horizontal plane [48]. To further improve the well-defined organization of tiny NPs of less than 10 nm into monolayered arrays, gold colloids are artificially confined in nanoscale grooves below a pipette, which can help to assemble parallel strips. The stacking layer of each strip is correlated with the groove's diameter; thus an NP monolayer with a tiny gap is fabricated within the tiny grooves [49]. Recently, it was demonstrated that self-assembly of an NP monolayer consisting of parallel strips can be switched on and off by precisely tailoring the contact angle of gold colloids on substrates across a critical value of 4.2° [50]. Whether and where the NP strips are created within a confined space on the micron scale depends on the magnitude of the contact angle, which can be quantitatively characterized by light interference (See Fig. 3) [50, 51].

Besides self-assembly within a confined volume, assembly of the colloidal NPs may be directed by templates with comparable feature sizes [52, 53]. Slightly tapered nanopillar arrays have been employed as the templates, since colloidal nanospheres can be deposited in the vacancies between adjacent nanopillars [54, 55]. Cui *et al.* delineated a practicable approach for the hierarchical assembly of isotropic and anisotropic colloidal nanostructures over large areas; this approach represents a significant step toward the integration of metallic colloids

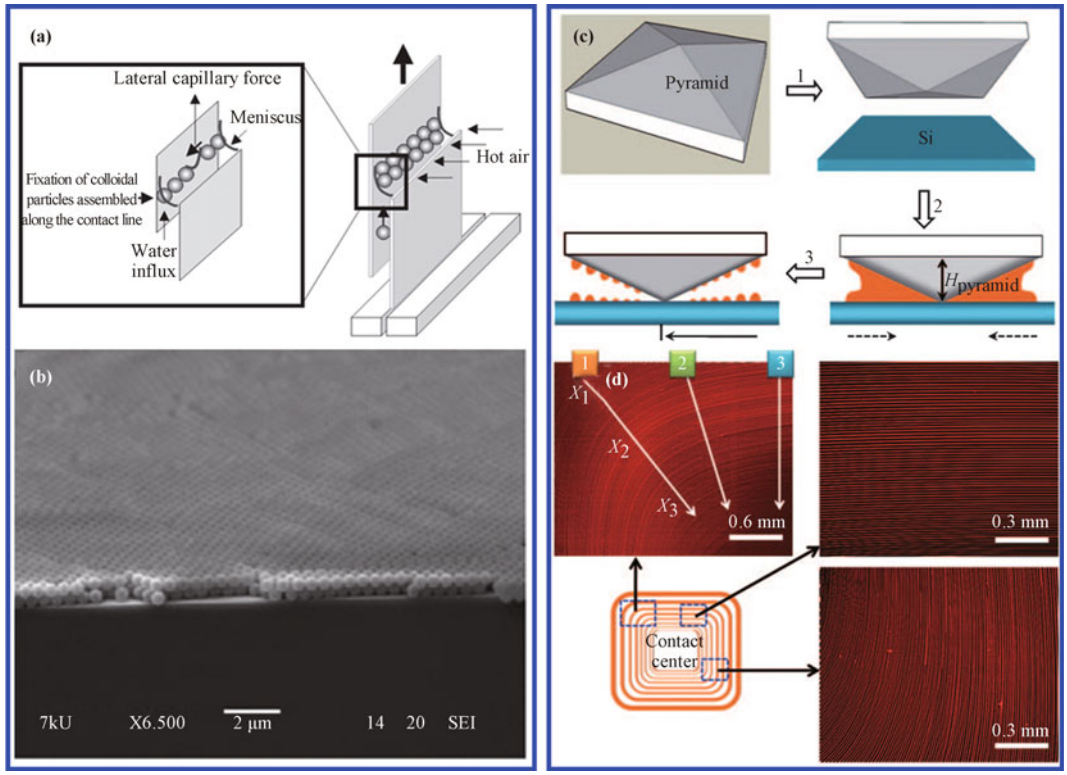

Fig. 2 Colloidal crystal films assembled at a confined volume. **(a)** Schematic illustration of small amount of colloidal suspension confined within two parallel glass sheets. **(b)** An SEM image of colloidal crystals. **(c)** Schematic illustration of the route for assembling the concentric square stripes below the indenter. **(d)** Typical fluorescence images, corresponding to the different locations defined in the lower left schematic, show the bent stripes and parallel straight stripes. The data in (a), (b), and (c), (d) were reproduced with permission from Refs. [46] and [47], respectively.

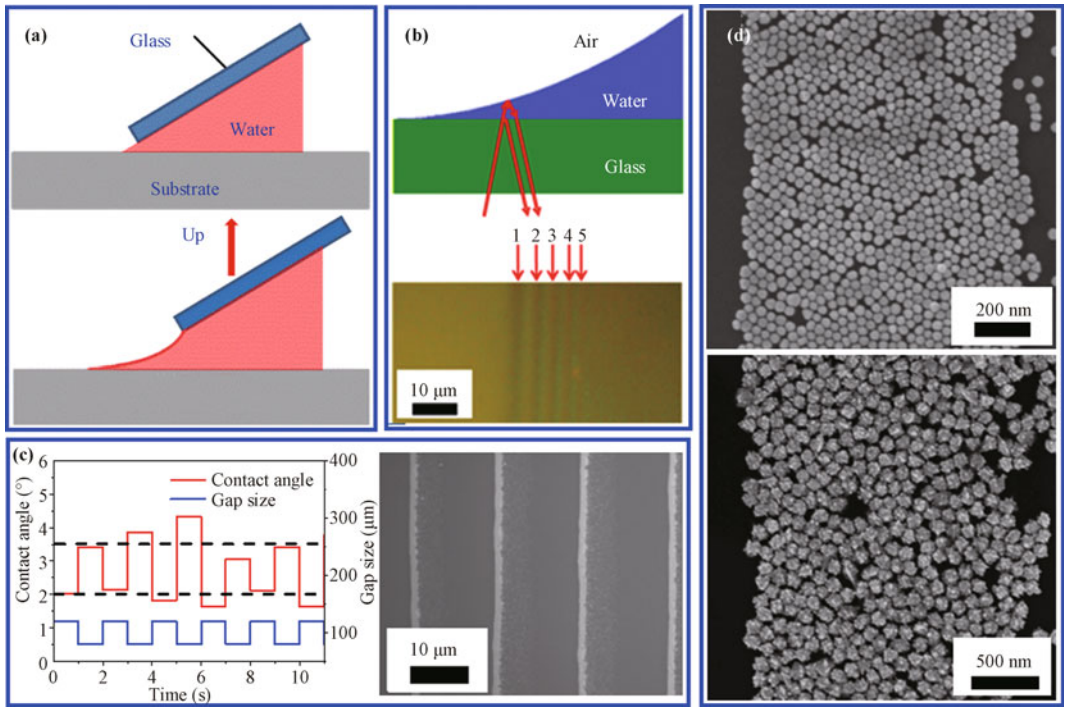

Fig. 3 Convective assembly at a confined contact angle. **(a)** Schematic illustration showing the tuning of the contact angle of the water confined between the substrate and the blade. **(b)** The schematic illustration of the generation of wedge interference when light is reflected at the air/water and water/glass interfaces. The interference pattern is collected in the vicinity of the contact line. **(c)** Alternate change of contact angle between 2° and 3.5°. **(d)** SEM images of the monolayered strips with spherical NPs and urchin-shape NPs. Reproduced with permission from Refs. [50] and [51].

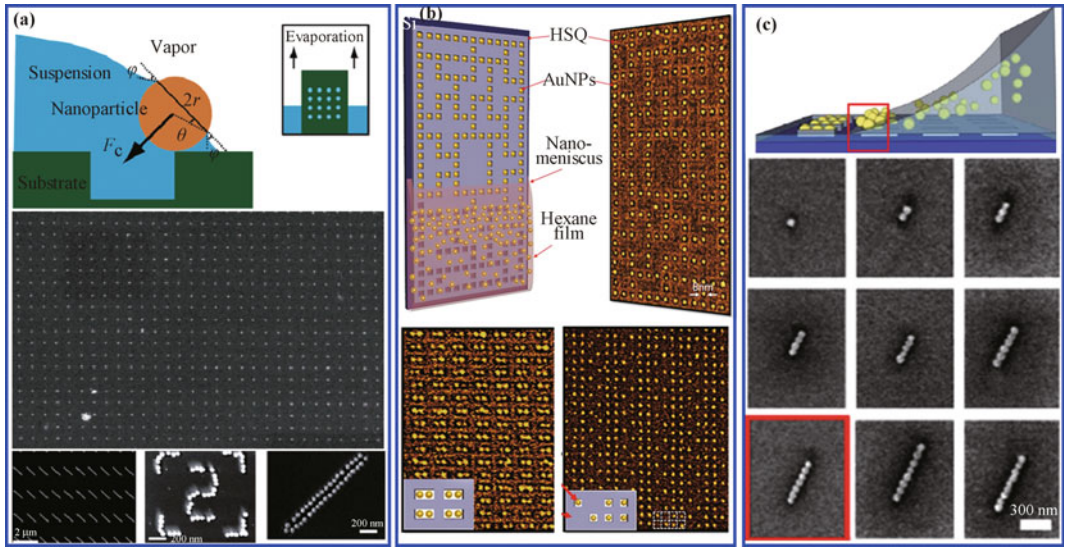

Fig. 4 Template-assisted self-assembly. **(a)** Schematic illustration of the capillary force assembly mechanism. SEM images of 50-nm-diameter Au NPs forming arrays on the templates. **(b)** Self-assembly of NPs with a diameter of 8 nm directed by the template. **(c)** Diagram of template-assisted self-assembly of NP chains with tunable lengths. Data in (a), (b), and (c) were reproduced with permission from Refs. [56], [57], and [26], respectively.

[See Fig. 4(a)] [56]. Asbahi *et al.* have pushed template-assisted self-assembly towards the use of sub-10 nm particles in the presence of surface topography. This process enables creating a thin liquid that confines NP dimers and NP chains because a moving nanomeniscus can, with precision, slot one single NP into the template [See Figs. 4(b) and (c)] [26, 57]. The advantages of this technique are its applicability to any type of NPs and quantum dots in principle and its capacity to be scaled up further to macroscopic areas through optimized coating processes and the precise control of assembling conditions [57]. The other driving force of self-assembly is an electric poten-

tial, in which the charged NPs move to an oppositely charged patterned electrode and are deposited selectively into a nanoscale cavity to create a two-dimensional pattern [58].

3 Tunable gaps at the sub-nm scale

As described above, the nanoscale gap can be reliably generated by self-assembly in a confined space. However, comparable and convincing optical properties should be collected only when the plasmonic gaps can be tuned in-situ with a spatial resolution in the sub-nm scale. This tunable feature is extremely important for the creation of "hot spots" for SERS applications and investigations of quantum plasmonics [59]. Normally, the gap size of the NP arrays situated on a flexible substrate can be tuned reliably by mechanical actuation, including mechanical bending, stretching, and compressing. This concept is experimentally valid in a variety of plasmonic structures supported by flexible substrates, including NP arrays [60], microvoids [61], cylindrical heptamers [62], and parallel gratings [63].

Mechanically stretching the elastomeric films is the simplest method to apply to tune the interparticle gaps without causing the deformation of the NPs. Han *et al.* observed the plasmonic shift of 1D Au NP chains by the plastic deformation of the polymer matrix. The shifting magnitude depends on the degree of mechanical deformation of the film. This novel NP film can be used to capture and to record the pressure distribution and magnitude by outputting color information that is quantified in a spectrometer [64]. Huang *et al.* demonstrated active plasmon tuning of individual Au NP dimers [See Fig. 5(a)]. This elastomeric method provides one route to tune interparticle separations at very short distances, thus optimizing the field enhancements at the interstitial spaces of two NPs for high SERS signals [28]. Alexander *et al.* developed a practicable method for controlling the spacing of nanorod dimers on silicone rubber [See Fig. 5(b)]. Subsequent measurements of the SERS enhancement factor over a range of interparticle separations yielded a trend consistent with what was predicted by theoretical simulations for primary mode resonances [65]. As a matter of fact, not only is mechanical stretching restricted for gap tuning in NP dimers, but also the ideal interstitial spacing can be controlled effectively in heptamer arrays, with the subsequent reliable shifts in Fano resonance [See Fig. 5(c)] [62].

In comparison with mechanical stretching, mechanically bending the substrate can offer precise control of a nanoscale gap within a relatively narrow range. Tian *et al.* claimed that a minimum gap size of 0.4 nm can be achieved; this is more sensitive than the tunable range in conventional stretching techniques. In our previous investigations, the gap within the NP monolayer can be tuned towards the sub-nm scale if the point of contact between the NPs and the polymer substrate is assumed [50, 66]. The minimum gap sizes reported in several researches are listed in Fig. 6 [27, 28, 34, 67]. In principle, uniform and reversible stretching (or compressing) of the flexible substrate will benefit the reliable tailoring of plasmonic gaps at the sub-nm scale. However, local deformation of the substrate relies significantly on its surface roughness, Poisson ratio, and the exact way to supply the loading. These restraining factors weaken the ability to tune the

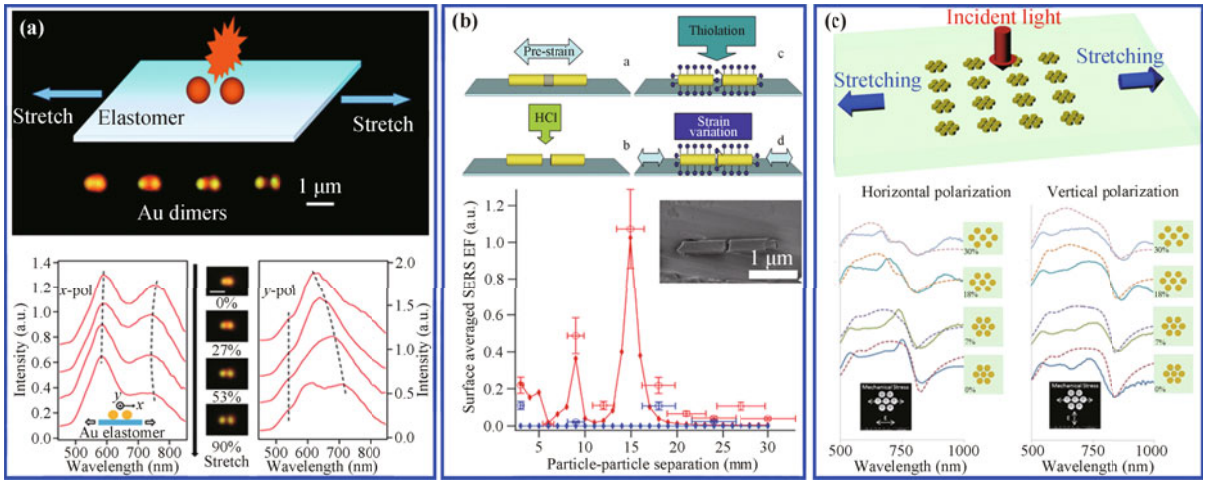

Fig. 5 Plasmonic gaps tuned by mechanical deformations. **(a)** Tunable dark-field scattering spectra of a single Au NP dimer. **(b)** Tunable Raman scattering of molecules absorbed onto the head-to-head nanorod dimer. Red and blue lines simulate results in transverse and perpendicular directions, respectively. Open diamond dots are experimental data. **(c)** Schematic illustration of gold heptamer arrays embedded in a polymer membrane, showing the tunable extinction spectra. Reproduced with permission from Refs. [28], [65], and [62].

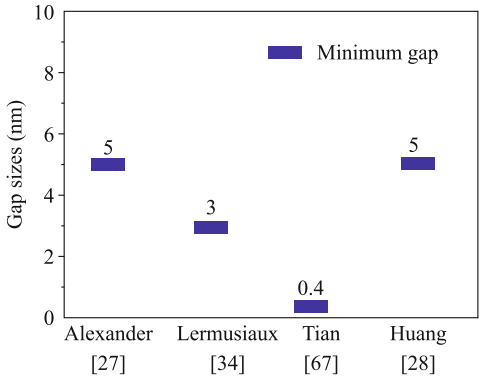

Fig. 6 Minimum limit of several plasmonic gaps tuned by mechanical stretching or mechanical bending. Reproduced with permission from Refs. [27], [28], [34], and [67].

gap at the sub-nm scale; so that the minimum gap achievable in this method is usually several nanometers, although the tuning range can reach tens of nanometers. In comparison with mechanical stretching and compressing, mechanical bending is a more efficient method for tailoring the sub-nm scale gap with fine steps. In this technique, the gap size depends on the strain level on the substrate's surface, which can be reversibly and reliably tuned by controlling its curvature during mechanical bending. Therefore, the surface roughness will not greatly affect the local curvature of the flexible substrate. The challenge here is the precise calculation of the local surface curvature, as our recent investigation has revealed [68]. It must be noted that the tuning range of plasmonic gaps is much smaller than the range during mechanical stretching and compressing.

4 Future perspectives

In theory, the sub-nm scale gap is a useful element for modeling and calculating quantum plasmons; experimental evidence for quantum effects in coupled NPs has also been acquired [69]. Yet there are several challenges to overcome in reliably tuning plasmonic gaps before a convincing quantitative theory can be formulated.

The exact gap size at which electron tunneling begins to appear has not been conclusively determined by the existing experimental results. Duan *et al.* suggested that the classic electrodynamics model only holds for gap sizes down to 0.5 nm in nanoprism dimmers [70]. However, both the electronic structures of the bridging molecules and the shape and local geometries of the junctions can affect the electrons' behaviors. This is reflected in the scattering spectrum and by electron energy loss spectroscopy [59, 71].

The second challenge emerges from the difficulty of obtaining precise characterizations and spectral measurements of plasmonic gaps in the sub-nm scale. Currently, transmission electron microscopy is still the main characterization method for observing gap size; its two-dimensional projections can lead to some errors, especially for NPs with some local changes in surface morphologies. The most reliable technique might lie in the capability for collecting projected images from different angles and then reconstructing a three-dimensional image of plasmonic gaps. If a plasmonic gap is tailored in-situ with a sub-nm step size, a series of spectra with excellent comparability can be collected at the different gaps. So far, although mechanical bending or stretching can in-situ change the gap size between the NPs, precise determination of the initial size and real-time evolution remain big experimental challenges. Recently, gap size evolution with the phase transition of a supporting substrate has been experimentally realized. This development might provide an alternative technique for tuning and characterizing the gaps in the transmission electron microscope in the future, where the supporting substrate is transparent to the electron beam [72]. In general, more precise control over the interparticle distances in the dimers is highly desired for introducing the optimal molecule linker, template, and solvent evaporation [73]. Meanwhile, precision in the characterization and tuning of gap size and real-time spectra collection is crucial for accelerating research on quantum plasmons and SERS in the near future [74].

Acknowledgements This work was partially supported by the Innovation Funding of HUST (Grant Nos. 2014ZZGH018 and 0118012074), the Specialized Research Fund for the Doctoral Program of Higher Education (Grant No. 20130142120089), and the National Natural Science Foundation of China (Grant Nos. 51371084 and 91545131).

References

1. C. B. Azzoni, D. D. I. Martino, V. Marchesi, B. Messiga, and M. P. Riccardi, Colour attributes of medieval window panes: Electron paramagnetic resonance and probe microanalyses on stained glass windows from Pavia-Carthusian monastery, *Archaeometry* 47(2), 381 (2005)
2. S. A. Maier and H. A. Atwater, Plasmonics: Localization and guiding of electromagnetic energy in metal/dielectric structures, *J. Appl. Phys.* 98(1), 011101 (2005)
3. G. Mie, Beiträge zur Optik trüber Medien, speziell kolloidaler Metallösungen, *Ann. Phys.* 330(3), 377 (1908)
4. N. J. Halas, S. Lal, W. S. Chang, S. Link, and P. Nordlander, Plasmons in strongly coupled metallic nanostructures, *Chem. Rev.* 111(6), 3913 (2011)
5. H. Raether, Surface Plasmons on Smooth and Rough Surfaces and on Gratings, Berlin: Springer, 1988

6. L. S. Jung, C. T. Campbell, T. M. Chinowsky, M. N. Mar, and S. S. Yee, Quantitative interpretation of the response of surface plasmon resonance sensors to adsorbed films, *Langmuir* 14(19), 5636 (1998)
7. B. Auguié and W. L. Barnes, Collective resonances in gold nanoparticle arrays, *Phys. Rev. Lett.* 101(14), 143902 (2008)
8. T. J. Yim, Y. Wang, and X. Zhang, Synthesis of a gold nanoparticle dimer plasmonic resonator through two-phase-mediated functionalization, *Nanotechnology* 19(43), 435605 (2008)
9. D. S. Kim, J. Heo, S. H. Ahn, S. W. Han, W. S. Yun, and Z. H. Kim, Real-space mapping of the strongly coupled plasmons of nanoparticle dimers, *Nano Lett.* 9(10), 3619 (2009)
10. S. Shen, L. Meng, Y. Zhang, J. Han, Z. Ma, S. Hu, Y. He, J. Li, B. Ren, T.M. Shih, Z. Wang, Z. Yang, and Z. Tian, Plasmon-enhanced second-harmonic generation nanorulers with ultrahigh sensitivities, *Nano Lett.* 15(10), 6716 (2015)
11. Z. Q. Tian and B. Ren, Adsorption and reaction at electrochemical interfaces as probed by surface-enhanced Raman spectroscopy, *Annu. Rev. Phys. Chem.* 55(1), 197 (2004)
12. E. C. Le Ru and P. G. Etchegoin, Single-molecule surface-enhanced Raman spectroscopy, *Annu. Rev. Phys. Chem.* 63(1), 65 (2012)
13. L. Li, T. Li, S. M. Wang, and S. N. Zhu, Collimated plasmon beam: Nondiffracting versus linearly focused, *Phys. Rev. Lett.* 110(4), 046807 (2013)
14. Y. J. Lu, J. Kim, H. Y. Chen, C. Wu, N. Dabidian, C. E. Sanders, C. Y. Wang, M. Y. Lu, B. H. Li, X. Qiu, W. H. Chang, L. J. Chen, G. Shvets, C. K. Shih, and S. Gwo, Plasmonic nanolaser using epitaxially grown silver film, *Science* 337(6093), 450 (2012)
15. A. V. Krasavin and A. V. Zayats, Photonic signal processing on electronic scales: Electro-optical field-effect nanoplasmonic modulator, *Phys. Rev. Lett.* 109(5), 053901 (2012)
16. M. L. Brongersma and V. M. Shalaev, The case for plasmonics, *Science* 328(5977), 440 (2010)
17. S. A. Maier, Plasmonics: Fundamentals and Applications, New York: Springer, 2007
18. W. S. Chang, J. B. Lassiter, P. Swanglap, H. Sobhani, S. Khatua, P. Nordlander, N. J. Halas, and S. Link, A plasmonic Fano switch, *Nano Lett.* 12(9), 4977 (2012)
19. A. V. Kabashin, P. Evans, S. Pastkovsky, W. Hendren, G. A. Wurtz, R. Atkinson, R. Pollard, V. A. Podolskiy, and A. V. Zayats, Plasmonic nanorod metamaterials for biosensing, *Nat. Mater.* 8(11), 867 (2009)
20. H. Wang, C. S. Levin, and N. J. Halas, Nanosphere arrays with controlled sub-10-nm gaps as surface-enhanced Raman spectroscopy substrates, *J. Am. Chem. Soc.* 127(43), 14992 (2005)
21. Z. Dong, M. Asbahi, J. Lin, D. Zhu, Y. M. Wang, K. Hippalgaonkar, H. S. Chu, W. P. Goh, F. Wang, Z. Huang, and J. K. W. Yang, Second-harmonic generation from sub-5 nm gaps by directed self-assembly of nanoparticles onto template-stripped gold substrates, *Nano Lett.* 15(9), 5976 (2015)
22. J. Y. Park, L. R. Baker, and G. A. Somorjai, Role of hot electrons and metal-oxide interfaces in surface chemistry and catalytic reactions, *Chem. Rev.* 115(8), 2781 (2015)
23. R. Esteban, A. Zugarramurdi, P. Zhang, P. Nordlander, F. J. García-Vidal, A. G. Borisov, and J. Aizpurua, A classical treatment of optical tunneling in plasmonic gaps: Extending the quantum corrected model to practical situations, *Faraday Discuss.* 178, 151 (2015)
24. C. Y. Li, J. C. Dong, X. Jin, S. Chen, R. Panneerselvam, A. V. Rudnev, Z. L. Yang, J. F. Li, T. Wandlowski, and Z. Q. Tian, In situ monitoring of electrooxidation processes at gold single crystal surfaces using shell-isolated nanoparticle-enhanced Raman spectroscopy, *J. Am. Chem. Soc.* 137(24), 7648 (2015)
25. L. M. Tong, H. X. Xu, and M. Käll, Nanogaps for SERS applications, *MRS Bull.* 39(2), 193 (2014)
26. K. D. Alexander, S. P. Zhang, A. R. Hight Walker, H. X. Xu, and R. Lopez, Relationship between length and surface-enhanced raman spectroscopy signal strength in metal nanoparticle chains: Ideal models versus nanofabrication, *J. Nanotechnol.* 2012, 840245 (2012)
27. K. D. Alexander, K. Skinner, S. Zhang, H. Wei, and R. Lopez, Tunable SERS in gold nanorod dimers through strain control on an elastomeric substrate, *Nano Lett.* 10(11), 4488 (2010)
28. F. Huang and J. J. Baumberg, Actively tuned plasmons on elastomerically driven Au nanoparticle dimers, *Nano Lett.* 10(5), 1787 (2010)
29. P. Dombi, A. Hörl, P. Rácz, I. Márton, A. Trügler, J. R. Krenn, and U. Hohenester, Ultrafast strong-field photoemission from plasmonic nanoparticles, *Nano Lett.* 13(2), 674 (2013)
30. R. Esteban, A. G. Borisov, P. Nordlander, and J. Aizpurua, Bridging quantum and classical plasmonics with a quantum-corrected model, *Nat. Commun.* 3, 825 (2012)
31. J. H. Yoon, Y. Zhou, M. G. Blaber, G. C. Schatz, and S. Yoon, Surface plasmon coupling of compositionally heterogeneous core-satellite nanoassemblies, *J. Phys. Chem. Lett.* 4(9), 1371 (2013)
32. J. H. Yoon, J. Lim, and S. Yoon, Controlled assembly and plasmonic properties of asymmetric core-satellite nanoassemblies, *ACS Nano* 6(8), 7199 (2012)
33. S. Aksu, M. Huang, A. Artar, A. A. Yanik, S. Selvarasah, M. R. Dokmeci, and H. Altug, Flexible plasmonics on unconventional and nonplanar substrates, *Adv. Mater.* 23(38), 4422 (2011)
34. L. Lermusiaux, V. Maillard, and S. Bidault, Widefield spectral monitoring of nanometer distance changes in DNA-templated plasmon rulers, *ACS Nano* 9(1), 978 (2015)
35. B. A. Grzybowski, C. E. Wilmer, J. Kim, K. P. Browne, and K. J. M. Bishop, Self-assembly: From crystals to cells, *Soft Matter* 5(6), 1110 (2009)

36. Z. M. Zhu, H. F. Meng, W. J. Liu, X. F. Liu, J. X. Gong, X. H. Qiu, L. Jiang, D. Wang, and Z. Y. Tang, Superstructures and SERS properties of gold nanocrystals with different shapes, *Angew. Chem. Int. Ed.* 50(7), 1593 (2011)
37. W. Cheng, M. J. Campolongo, J. J. Cha, S. J. Tan, C. C. Umbach, D. A. Muller, and D. Luo, Free-standing nanoparticle superlattice sheets controlled by DNA, *Nat. Mater.* 8(6), 519 (2009)
38. M. P. Cecchini, V. A. Turek, J. Paget, A. A. Kornyshev, and J. B. Edel, Self-assembled nanoparticle arrays for multiphase trace analyte detection, *Nat. Mater.* 12(2), 165 (2013)
39. L. Shao, C. Fang, H. Chen, Y. C. Man, J. Wang, and H. Q. Lin, Distinct plasmonic manifestation on gold nanorods induced by the spatial perturbation of small gold nanospheres, *Nano Lett.* 12(3), 1424 (2012)
40. Z. Yang, S. Chen, P. Fang, B. Ren, H. H. Girault, and Z. Tian, LSPR properties of metal nanoparticles adsorbed at a liquid-liquid interface, *Phys. Chem. Chem. Phys.* 15(15), 5374 (2013)
41. H. Liu, Z. Yang, L. Meng, Y. Sun, J. Wang, L. Yang, J. Liu, and Z. Tian, Three-dimensional and time-ordered surface-enhanced Raman scattering hotspot matrix, *J. Am. Chem. Soc.* 136(14), 5332 (2014)
42. J. Chen, B. Shen, G. Qin, X. Hu, L. Qian, Z. Wang, S. Li, Y. Ren, and L. Zuo, Fabrication of large-area, high-enhancement SERS substrates with tunable interparticle spacing and application in identifying microorganisms at the single cell level, *J. Phys. Chem. C* 116(5), 3320 (2012)
43. Z. Dai, Y. Li, G. Duan, L. Jia, and W. Cai, Phase diagram, design of monolayer binary colloidal crystals, and their fabrication based on ethanol-assisted self-assembly at the air/water interface, *ACS Nano* 6(8), 6706 (2012)
44. R. D. Deegan, O. Bakajin, T. F. Dupont, G. Huber, S. R. Nagel, and T. A. Witten, Capillary flow as the cause of ring stains from dried liquid drops, *Nature* 389(6653), 827 (1997)
45. A. S. Dimitrov and K. Nagayama, Continuous convective assembling of fine particles into two-dimensional arrays on solid surfaces, *Langmuir* 12(5), 1303 (1996)
46. M. H. Kim, S. H. Im, and O. O. Park, Rapid fabrication of two- and three-dimensional colloidal crystal films via confined convective assembly, *Adv. Funct. Mater.* 15(8), 1329 (2005)
47. S. W. Hong, M. Byun, and Z. Q. Lin, Robust self-assembly of highly ordered complex structures by controlled evaporation of confined microfluids, *Angew. Chem. Int. Ed.* 48(3), 512 (2009)
48. L. H. Qian and R. Mookherjee, Convective assembly of linear gold nanoparticle arrays at the micron scale for surface enhanced Raman scattering, *Nano Res.* 4(11), 1117 (2011)
49. L. H. Qian, S. J. Zhai, Y. T. Jiang, and B. Das, Nanoscale convection assisted self-assembly of nanoparticle monolayer, *J. Mater. Chem.* 22(11), 4932 (2012)
50. C. Zhang, J. Li, S. Yang, W. Jiao, S. Xiao, M. Zou, S. Yuan, F. Xiao, S. Wang, and L. Qian, Closely packed nanoparticle monolayer as a strain gauge fabricated by convective assembly at a confined angle, *Nano Res.* 7(6), 824 (2014)
51. L. Z. Yi, W. H. Jiao, K. Wu, L. H. Qian, X. X. Yu, Q. Xia, K. M. Mao, S. L. Yuan, S. Wang, and Y. T. Jiang, Nanoparticle monolayer-based flexible strain gauge with ultrafast dynamic response for acoustic vibration detection, *Nano Res.* 8(9), 2978 (2015)
52. J. Zhang, Y. Li, X. Zhang, and B. Yang, Colloidal self-assembly meets nanofabrication: from two-dimensional colloidal crystals to nanostructure arrays, *Adv. Mater.* 22(38), 4249 (2010)
53. M. Asbahi, S. Mehraeen, K. T. P. Lim, F. Wang, J. Cao, M. C. Tan, and J. K. W. Yang, Template-induced structure transition in sub-10 nm self-assembling nanoparticles, *Nano Lett.* 14(5), 2642 (2014)
54. C. Jin, M. A. McLachlan, D. W. McComb, R. M. De La Rue, and N. P. Johnson, Template-assisted growth of nominally cubic (100)-oriented three-dimensional crack-free photonic crystals, *Nano Lett.* 5(12), 2646 (2005)
55. C. J. Jin, Z. Y. Li, M. A. McLachlan, D. W. McComb, R. M. De La Rue, and N. P. Johnson, Optical properties of tetragonal photonic crystal synthesized via template-assisted self-assembly, *J. Appl. Phys.* 99(11), 116109 (2006)
56. Y. Cui, M. T. Björk, J. A. Liddle, C. Sönnichsen, B. Boussert, and A. P. Alivisatos, Integration of colloidal nanocrystals into lithographically patterned devices, *Nano Lett.* 4(6), 1093 (2004)
57. M. Asbahi, S. Mehraeen, F. Wang, N. Yakovlev, K. S. L. Chong, J. Cao, M. C. Tan, and J. K. W. Yang, Large area directed self-assembly of sub-10 nm particles with single particle positioning resolution, *Nano Lett.* 15(9), 6066 (2015)
58. A. Pescaglini, A. O'Riordan, A. J. Quinn, and D. Iacopino, Controlled assembly of Au nanorods into 1D architectures by electric field assisted deposition, *J. Mater. Chem. C* 2(33), 6810 (2014)
59. H. Cha, J. H. Yoon, and S. Yoon, Probing quantum plasmon coupling using gold nanoparticle dimers with tunable interparticle distances down to the subnanometer range, *ACS Nano* 8(8), 8554 (2014)
60. S. Malynych and G. Chumanov, Light-induced coherent interactions between silver nanoparticles in two-dimensional arrays, *J. Am. Chem. Soc.* 125(10), 2896 (2003)
61. R. M. Cole, S. Mahajan, and J. J. Baumberg, Stretchable metal-elastomer nanovoids for tunable plasmons, *Appl. Phys. Lett.* 95(15), 154103 (2009)
62. Y. Cui, J. Zhou, V. A. Tamma, and W. Park, Dynamic tuning and symmetry lowering of Fano resonance in plasmonic nanostructure, *ACS Nano* 6(3), 2385 (2012)
63. S. Olcum, A. Kocabas, G. Ertas, A. Atalar, and A. Aydinli, Tunable surface plasmon resonance on an elastomeric substrate, *Opt. Express* 17(10), 8542 (2009)
64. X. Han, Y. Liu, and Y. Yin, Colorimetric stress memory sensor based on disassembly of gold nanoparticle chains, *Nano Lett.* 14(5), 2466 (2014)

65. K. D. Alexander, K. Skinner, S. Zhang, H. Wei, and R. Lopez, Tunable SERS in gold nanorod dimers through strain control on an elastomeric substrate, *Nano Lett.* 10(11), 4488 (2010)

66. W. Jiao, L. Yi, C. Zhang, K. Wu, J. Li, L. Qian, S. Wang, Y. Jiang, B. Das, and S. Yuan, Electrical conduction of nanoparticle monolayer for accurate tracking of mechanical stimulus in finger touch sensing, *Nanoscale* 6(22), 13809 (2014)

67. J. H. Tian, B. Liu, X. Li, Z. L. Yang, B. Ren, S. T. Wu, N. Tao, and Z. Q. Tian, Study of molecular junctions with a combined surface-enhanced Raman and mechanically controllable break junction method, *J. Am. Chem. Soc.* 128(46), 14748 (2006)

68. L. Z. Yi, W. H. Jiao, C. M. Zhu, K. Wu, C. Zhang, L. H. Qian, S. Wang, Y. T. Jiang, and S. L. Yuan, *Nano Res.* (2016) (in press)

69. K. J. Savage, M. M. Hawkeye, R. Esteban, A. G. Borisov, J. Aizpurua, and J. J. Baumberg, Revealing the quantum regime in tunnelling plasmonics, *Nature* 491(7425), 574 (2012)

70. H. Duan, A. I. Fernández-Domínguez, M. Bosman, S. A. Maier, and J. K. W. Yang, Nanoplasmonics: Classical down to the nanometer scale, *Nano Lett.* 12(3), 1683 (2012)

71. S. F. Tan, L. Wu, J. K. W. Yang, P. Bai, M. Bosman, and C. A. Nijhuis, Quantum plasmon resonances controlled by molecular tunnel junctions, *Science* 343(6178), 1496 (2014)

72. S. K. Earl, T. D. James, T. J. Davis, J. C. McCallum, R. E. Marvel, Haglund, and A. Roberts, Tunable optical antennas enabled by the phase transition in vanadium dioxide, *Opt. Express* 21(22), 27503 (2013)

73. L. P. Xia, Z. Yang, S. Y. Yin, W. R. Guo, J. L. Du, and C. L. Du, Hole arrayed metal-insulator-metal structure for surface enhanced Raman scattering by self-assembling polystyrene spheres, *Front. Phys.* 9(1), 68 (2014)

74. Z. L. Zhang, L. Chen, S. X. Sheng, M. T. Sun, H. R. Zheng, K. Q. Chen, and H. X. Xu, High-vacuum tip enhanced Raman spectroscopy, *Front. Phys.* 9(1), 24 (2014)